



OPEN

## Entropy optimized dissipative flow of hybrid nanofluid in the presence of non-linear thermal radiation and Joule heating

Wei-Feng Xia<sup>1</sup>, M. U. Hafeez<sup>2</sup>, M. Ijaz Khan<sup>3,4</sup>, Nehad Ali Shah<sup>5,6</sup>✉ & Jae Dong Chung<sup>5</sup>

Present article reads three dimensional flow analysis of incompressible viscous hybrid nanofluid in a rotating frame. Ethylene glycol is used as a base liquid while nanoparticles are of copper and silver. Fluid is bounded between two parallel surfaces in which the lower surface stretches linearly. Fluid is conducting hence uniform magnetic field is applied. Effects of non-linear thermal radiation, Joule heating and viscous dissipation are entertained. Interesting quantities namely surface drag force and Nusselt number are discussed. Rate of entropy generation is examined. Bvp4c numerical scheme is used for the solution of transformed O.D.Es. Results regarding various flow parameters are obtained via bvp4c technique in MATLAB Software version 2019, and displayed through different plots. Our obtained results presents that velocity field decreases with respect to higher values of magnetic parameter, Reynolds number and rotation parameter. It is also observed that the temperature field boots subject to radiation parameter. Results are compared with Ishak et al. (Nonlinear Anal R World Appl 10:2909–2913, 2009) and found very good agreement with them. This agreement shows that the results are 99.99% match with each other.

Boundary layer flow over a stretched surface has a key importance in both experimental and theoretical point of views. When surface stretches with certain velocity, it develops an in viscid flow immediately, but the viscous flow near the sheet improves slowly, and it takes a certain instant of time to become a fully developed steady flow. Hayat et al.<sup>1</sup> studied the flow of Maxwell fluid over a stretching surface. Andersson et al.<sup>2</sup> examined the viscoelastic and electrically conducting flow over a stretching sheet. Kabir et al.<sup>3</sup> discussed the mechanism of heat and mass transfer of power law fluid past a stretching sheet in the presence of chemical reaction and radiation effects.

Fastest mode of thermal transport is radiation in which heat transfers in the form of electromagnetic waves without any dependency of medium. Hayat et al.<sup>4</sup> analyzed the effects of non-linear thermal radiation on the entropy optimized flow. Shehzad et al.<sup>5</sup> addressed the thermal transport mechanism of Jeffrey nanofluid flow in the presence of non-linear thermal radiation. Waqas et al.<sup>6</sup> investigated the flow on slandering stretching surface by encountering the effects of thermophoresis, Brownian diffusion and non-linear radiation. Kumar et al.<sup>7</sup> studied the flow of nanofluid over a stretched surface with non-linear radiation and chemical reaction.

Presence of shear forces reasons the work done by the fluid on its adjacent layers and in irreversible processes this work done transfers into heat. This whole thermodynamic process is termed as viscous dissipation. Gebhart et al.<sup>8</sup> analyzed the dissipative effects in natural convection. Koo et al.<sup>9</sup> explored the impact of viscous dissipation in micro channels and tubes. Flow of magneto-nanofluid in the presence of viscous dissipation is carried out by Hayat et al.<sup>10</sup>. Mustafa et al.<sup>11</sup> presented the study of Jeffrey fluid near the stagnation point by considering the dissipative effects.

A thermodynamic term highly associated with irreversible processes is called entropy. This term is deducted from second law of thermodynamics. Entropy calculates the rate disorder and randomness of the system. Bejan et al.<sup>12</sup> investigated the role of entropy in thermal transport mechanism. Rashidi et al.<sup>13</sup> presented entropy

<sup>1</sup>School of Engineering, Huzhou University, Huzhou 313000, People's Republic of China. <sup>2</sup>Department of Mathematics, Quaid-I-Azam University 45320, Islamabad 44000, Pakistan. <sup>3</sup>Department of Mathematics and Statistics, Riphah International University I-14, Islamabad 44000, Pakistan. <sup>4</sup>Nonlinear Analysis and Applied Mathematics (NAAM)-Research Group, Department of Mathematics, Faculty of Sciences, King Abdulaziz University, P.O. Box 80203, Jeddah 21589, Saudi Arabia. <sup>5</sup>Department of Mechanical Engineering, Sejong University, Seoul 05006, Korea. <sup>6</sup>Department of Mathematics, Lahore Leads University, Lahore, Pakistan. ✉email: nehadali199@yahoo.com

Nanoparticles/base fluid	$k(W/mK)$	$\rho(kg/m^3)$	$\sigma(s/m)$	$c_p(J/kgM)$
Silver (Ag)	429	10,500	$6.30 * 10^7$	235
Copper (Cu)	401	8933	$5.96 * 10^7$	385
Ethylene glycol (EG)	0.253	1115	$1.10 * 10^{-4}$	2430

**Table 1.** Transport characteristics of base fluid and nanoparticles<sup>22,23</sup>.

Pr	Ishak et al. <sup>21</sup>	Present work
0.72	0.809	0.806
1.0	1.000	1.000
3.0	1.924	1.923
10.0	3.721	3.720

**Table 2.** Comparative analysis of Nusselt number for different values of Prandtl number when remaining parameters of temperature equation is zero.

optimized flow of electrically conducting nanofluid. Hayat et al.<sup>14</sup> explained entropy impact on flow containing copper and silver nanoparticles.

Heat transfer fluids have very important applications at industrial sides. Since base liquid are bad conductors of heat due to their weak thermal properties hence the heat transfer devices were less efficient. Here nanotechnology played a key role; Choi<sup>15</sup> was the first to utilize the term nanofluid. He prepared it by inserting nanoparticles in ordinary liquid and he proved the enhancement in thermal transport process. After that, many of the researchers adopted that technique and many experimental and theoretical work were done in this regard. Prasher et al.<sup>16</sup> presented the brief study of thermal and viscous properties of nanofluid. Sheikholeslami et al.<sup>17</sup> discussed MFD viscosity effects of mixed convective magneto-nanofluid. New classification of nanotechnology is hybrid nanofluid with enhanced thermal properties. This nanomaterial is consists of two or more than two nanoparticles in ordinary liquid and the obtained results are more powerful than that of nanofluid. Khan et al.<sup>18</sup> explored the MHD containing rotating flow of hybrid nanofluid with entropy generation. Chamkha et al.<sup>19</sup> presented the study of hybrid nanofluid in the presence of radiation and Joule heating. Hayat et al.<sup>20</sup> studied heat transfer enhancement in the flow of hybrid nanofluid.

Our main target in this research work is to examine the transport characteristics of three different types of hybrid nanoparticles i.e., Ethylene Glycol, Copper and Silver in magnetohydrodynamic flow of viscous fluid between two parallel moving surfaces. The considered fluid is electrical conducting subject to applied magnetic field and bounded between two parallel surfaces in which lower surface linearly stretches. Whole system obeys uniform rotation along specified direction. Energy equation includes conduction, non-linear radiation, Ohmic heating and viscous dissipation. According to author observation, no such attempt is yet done on such topic in literature. Entropy rate is calculated. Graphical analysis of surface drag force and Nusselt number are addressed. Transformations are used to convert the non-linear PDEs to ODEs. Bvp4c Numerical approach is used for the solution of transformed system. Table 1 shows the thermo-physical values of base liquid and nanoparticles. Table 2 presents the comparative result of present work with Ishak et al.<sup>21</sup>.

Some latest literature on fluid flow behavior towards a different geometries is listed in Refs.<sup>24–30</sup>.

## Problem statement

Here we are considering incompressible, steady and viscous flow of hybrid nanofluid bounded between two parallel surfaces which are  $D$  distant apart. In hybrid nanomixture, Ethylene glycol (EG) act as a base liquid while copper (Cu) and silver (Ag) as nanoparticles. Since fluid is electromagnetically conducting, hence constant magnetic field  $B_0$  is applied along  $y$  direction by ignoring the electric field effects. There is linear stretching surface at  $y = 0$  with stretching velocity  $cx$ . The considered system is rotating with constant angular velocity  $\Omega$  along  $y$  direction. Figure 1 shows the physical appearance of the problem.

Mathematical form of the modeled problem is<sup>23</sup>:

$$\frac{\partial u}{\partial x} + \frac{\partial v}{\partial y} = 0, \quad (1)$$

$$u \frac{\partial u}{\partial x} + v \frac{\partial u}{\partial y} + 2\Omega w = -\frac{1}{\rho_{hmf}} \frac{\partial p}{\partial x} + \frac{\mu_{hmf}}{\rho_{hmf}} \left( \frac{\partial^2 u}{\partial x^2} + \frac{\partial^2 u}{\partial y^2} \right) - \frac{\sigma_{hmf} B_0^2}{\rho_{hmf}} u, \quad (2)$$

$$u \frac{\partial v}{\partial x} + v \frac{\partial v}{\partial y} = -\frac{1}{\rho_{hmf}} \frac{\partial p}{\partial y} + \frac{\mu_{hmf}}{\rho_{hmf}} \left( \frac{\partial^2 v}{\partial x^2} + \frac{\partial^2 v}{\partial y^2} \right), \quad (3)$$

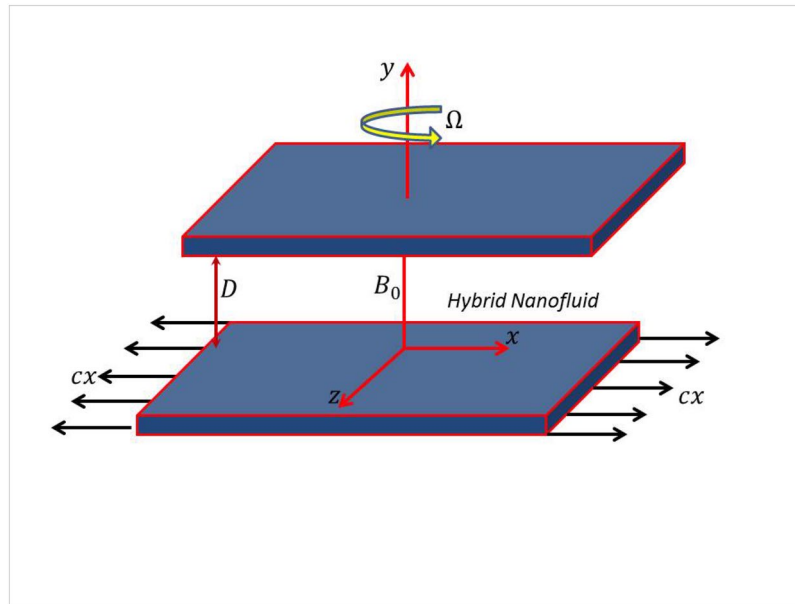


**Figure 1.** Graphical abstract.

$$u \frac{\partial w}{\partial x} + v \frac{\partial w}{\partial y} - 2\Omega u = \frac{\mu_{hnf}}{\rho_{hnf}} \left( \frac{\partial^2 w}{\partial x^2} + \frac{\partial^2 w}{\partial y^2} \right) - \frac{\sigma_{hnf} B_0^2}{\rho_{hnf}} w, \tag{4}$$

$$\left. \begin{aligned} u \frac{\partial T}{\partial x} + v \frac{\partial T}{\partial y} = & \frac{k_{hnf}}{(\rho c_p)_{hnf}} \left( \frac{\partial^2 T}{\partial x^2} + \frac{\partial^2 T}{\partial y^2} \right) - \frac{1}{(\rho c_p)_{hnf}} \frac{\partial q_r}{\partial y} + \frac{\sigma_{hnf} B_0^2}{(\rho c_p)_{hnf}} (u^2 + w^2) \\ & + \frac{\mu_{hnf}}{(\rho c_p)_{hnf}} \left( 2 \left( \frac{\partial u}{\partial x} \right)^2 + 2 \left( \frac{\partial v}{\partial y} \right)^2 + \left( \frac{\partial u}{\partial y} \right)^2 + \left( \frac{\partial w}{\partial x} \right)^2 + \left( \frac{\partial w}{\partial y} \right)^2 \right). \end{aligned} \right\} \tag{5}$$

On the R.H.S of Eq. (5), first term is due to conduction, second term is due to radiation, third term is due to Joule heating and last term represents the viscous dissipation. By Rosseland’s approximation, the non-linear radiative heat flux  $q_r$  is given as,

$$q_r = - \frac{16\sigma^* T^3}{3k^*} \frac{\partial T}{\partial y}. \tag{6}$$

The boundary conditions for the present flow satisfy

$$\left. \begin{aligned} u = cx, \quad v = 0, \quad w = 0, \quad T = T_0 \text{ at } y = 0, \\ u = 0, \quad v = 0, \quad w = 0, \quad T = T_L \text{ at } y = D. \end{aligned} \right\} \tag{7}$$

Here  $x, y$  highlights Cartesian coordinates,  $u, v, w$  the velocity components,  $c$  the stretching rate,  $p$  pressure,  $\rho_{hnf}$  density,  $T$  temperature,  $\sigma_{hnf}$  electrical conductivity,  $\sigma^*$  Stefan Boltzmann constant,  $\mu_{hnf}$  dynamic viscosity,  $k^*$  mean absorption coefficient,  $\Omega$  angular frequency,  $(\rho c_p)_{hnf}$  heat capacity,  $k_{hnf}$  thermal conductivity. Due to net crossflow along  $z - axis$ ,  $\frac{\partial p}{\partial z}$  is absent in Eq. (4). The subscript  $hnf$  represents hybrid nanofluid.

Thermo-physical aspects of hybrid nanofluid

Hybrid nanofluid dynamic viscosity is given by

$$\frac{\mu_{hnf}}{\mu_f} = \frac{1}{(1 - \phi_{Cu} - \phi_{Ag})^{2.5}}. \tag{8}$$

Density of hybrid nanofluid obeys

$$\frac{\rho_{hnf}}{\rho_f} = (1 - \phi_{Cu} - \phi_{Ag}) + \frac{\phi_{Cu} \rho_{Cu} + \phi_{Ag} \rho_{Ag}}{\rho_f}. \tag{9}$$

Heat capacity of hybrid nanofluid satisfies

$$\frac{(\rho c_p)_{hnf}}{(\rho c_p)_f} = (1 - \phi_{Cu} - \phi_{Ag}) + \phi_{Cu} (\rho c_p)_{Cu} + \phi_{Ag} (\rho c_p)_{Ag}. \tag{10}$$

Thermal conductivity of hybrid nanofluid is

$$\frac{k_{hnf}}{k_f} = \frac{\left(\frac{\phi_{Cu}k_{Cu} + \phi_{Ag}k_{Ag}}{\phi_{Cu} + \phi_{Au}} + 2k_f + 2(\phi_{Cu}k_{Cu} + \phi_{Ag}k_{Ag}) - 2(\phi_{Cu} + \phi_{Ag})k_f\right)}{\left(\frac{\phi_{Cu}k_{Cu} + \phi_{Ag}k_{Ag}}{\phi_{Cu} + \phi_{Ag}} + 2k_f - (\phi_{Cu}k_{Cu} + \phi_{Ag}k_{Ag}) - (\phi_{Cu} + \phi_{Ag})k_f\right)}. \quad (11)$$

Hybrid nanofluid electrical conductivity yield

$$\frac{\sigma_{hnf}}{\sigma_f} = 1 + \frac{3\left(\frac{\phi_{Cu}\sigma_{Cu} + \phi_{Ag}\sigma_{Ag}}{\sigma_f} - (\phi_{Cu} + \phi_{Ag})\right)}{\left(\frac{\phi_{Cu}\sigma_{Cu} + \phi_{Ag}\sigma_{Ag}}{\sigma_f} + 2\right) - \left(\frac{\phi_{Cu}\sigma_{Cu} + \phi_{Ag}\sigma_{Ag}}{\sigma_f} - (\phi_{Cu} + \phi_{Ag})\right)}. \quad (12)$$

Here we have used equal volume concentration of nanoparticles ( $\phi_{Cu} = \phi_{Ag} = 0.5\phi$ ).

## Transformation procedure

Here we are considering the following variables

$$\left. \begin{aligned} u &= cx f'(\eta), \quad v = -cDf(\eta), \quad w = cxg(\eta), \\ \theta &= \frac{T - T_0}{T_D - T_0}, \quad \eta = \frac{y}{D}. \end{aligned} \right\}. \quad (13)$$

Conservation law of mass (Eq. 1) is trivially satisfied and the other flow equations yield

$$f^{iv} + Re \frac{N_2}{N_1} (ff''' - f'f'') - 2Ro \frac{N_2}{N_1} g' - Mn \frac{N_5}{N_1} f'' = 0, \quad (14)$$

$$g'' + Re \frac{N_2}{N_1} (fg' - f'g) + 2Ro \frac{N_2}{N_1} f' - Mn \frac{N_5}{N_1} g = 0, \quad (15)$$

$$\left. \begin{aligned} [N_4 + R(1 + (\theta_w - 1)\theta)^3] \theta'' + N_3 \text{Pr} \text{Re} f \theta' + 3R(\theta_w - 1)(1 + (\theta_w - 1)\theta)^2 \theta'^2 \\ + N_1 \text{Pr} [Ec_D(4f'^2 + g^2) + Ec_x(f''^2 + g'^2)] + N_5 Mn Ec_x \text{Pr} \text{Re} (f'^2 + g^2) = 0, \end{aligned} \right\} \quad (16)$$

$$\left. \begin{aligned} f(0) = 0, \quad f'(0) = 1, \quad g(0) = 0, \quad \theta(0) = 1 \text{ at } \eta = 0, \\ f(1) = 0, \quad f'(1) = 0, \quad g(1) = 0, \quad \theta(1) = 0 \text{ at } \eta = 1. \end{aligned} \right\} \quad (17)$$

Here  $\theta_w = \left(\frac{T_0}{T_D}\right)$  temperature ratio parameter ( $T_0 > T_D$ ),  $Re = \left(\frac{cD^2 \rho_f}{\mu_f}\right)$  Reynolds number,  $\text{Pr} = \left(\frac{\mu_f c_{pf}}{k_f}\right)$  Prandtl number,  $Mn = \left(\frac{\sigma_f B_0^2 D^2}{\mu_f}\right)$  magnetic parameter,  $R = \left(\frac{16\sigma^* T_D}{3k^* k_f}\right)$  radiation parameter,  $Ro = \left(\frac{\Omega D^2 \rho_f}{\mu_f}\right)$  rotation parameter,  $Ec_x = \left(\frac{c^2 x^2}{c_{pf} T_D (\theta_w - 1)}\right)$  and  $Ec_D = \left(\frac{c^2 D^2}{c_{pf} T_D (\theta_w - 1)}\right)$  are the Eckert numbers.  $N_1, N_2, N_3, N_4$  and  $N_5$  are mathematically given as

$$N_1 = \frac{\mu_{hnf}}{\mu_f}, \quad N_2 = \frac{\rho_{hnf}}{\rho_f}, \quad N_3 = \frac{(\rho c_p)_{hnf}}{(\rho c_p)_f}, \quad N_4 = \frac{k_{hnf}}{k_f} \text{ and } N_5 = \frac{\sigma_{hnf}}{\sigma_f} \quad (18)$$

## Entropy generation

Rate of entropy generation is defined as

$$\left. \begin{aligned} E_G &= \frac{\mu_{hnf}}{T_D} \left[ 2\left(\frac{\partial u}{\partial x}\right)^2 + 2\left(\frac{\partial v}{\partial y}\right)^2 + \left(\frac{\partial u}{\partial y}\right)^2 + \left(\frac{\partial w}{\partial x}\right)^2 + \left(\frac{\partial w}{\partial y}\right)^2 \right] \\ &+ \frac{k_f}{T_D^2} \left[ \frac{k_{hnf}}{k_f} + \frac{16\sigma^* T^3}{3k^* k^*} \right] \left( \left(\frac{\partial T}{\partial x}\right)^2 + \left(\frac{\partial T}{\partial y}\right)^2 \right) + \frac{\sigma_{hnf}}{T_D} B_0^2 (u^2 + w^2), \end{aligned} \right\} \quad (19)$$

after applying the transformations, entropy generation becomes

$$Ng = \frac{E_G}{E_{Go}} = N_1 Ec_D \text{Pr} (4f'^2 + g^2) + N_1 Ec_x \text{Pr} (f''^2 + g'^2) + \left( N_4 + R(1 + (\theta_w - 1)\theta)^3 \right) \theta'^2 + N_5 Mn \text{Pr} Ec_x (f'^2 + g^2). \quad (20)$$

where  $E_{Go} = \left(\frac{k_f(\theta_w - 1)}{D^2}\right)$  is the characteristics entropy generation.

## Physical quantities

**Surface drag force.** Expression of surface drag force satisfies

$$C_f^* = \frac{-2\tau_w}{\rho_{hnf}(cx)^2}, \quad (21)$$

where

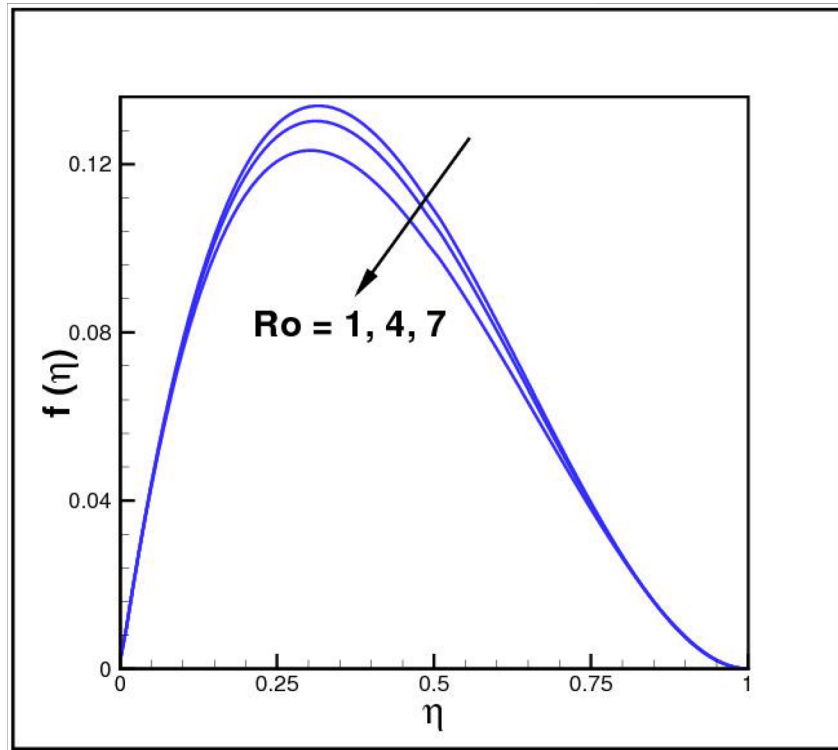


**Figure 2.** Impact of  $Ro$  on  $f(\eta)$ .

$$\tau_w = \mu_{hnf} \frac{\partial u}{\partial y} \Big|_{y=D}, \tag{22}$$

or scalar form is

$$C_f Re_x = -2 \frac{N_1}{N_2} f''(1). \tag{23}$$

**Nusselt number.** Mathematically one has

$$Nu^* = \frac{Dq_w}{k_f(T_D - T_0)(\theta_w - 1)}, \tag{24}$$

where

$$q_w = - \left[ k_{hnf} + \frac{16\sigma^* T^3}{3k^*} \right] \frac{\partial T}{\partial y} \Big|_{y=D}, \tag{25}$$

The final form is

$$Nu = - [N_4 + R(1 + (\theta_w - 1)\theta(1))^3] \theta'(1). \tag{26}$$

### Discussion

Here the dissipative flow of hybrid nanofluid with entropy generation is discussed. Impact of interesting parameters namely magnetic parameter  $Mn$ , rotation parameter  $Ro$ , Reynolds number  $Re$ , temperature ratio parameter  $\theta_w$ , radiation parameter  $R$ , and Eckert number  $Ec_x$  are examined.

Figures 2, 3 and 4 present the influences of rotation parameter  $Ro$ , Reynolds number  $Re$  and magnetic parameter  $Mn$  on velocity component  $f(\eta)$ , respectively. Here  $f(\eta)$  is decreasing function of all such parameters. Physically more  $Mn$  produces more Lorentz force which offers resistance to flow. Figures 5 and 6 portray the impacts of  $Ro$  and  $Mn$  on velocity profile  $g(\eta)$ , higher values of both parameters reasons the enhancement in  $g(\eta)$ , while opposite trend is noted for Reynolds number  $Re$ , here higher  $Re$  declines the velocity  $g(\eta)$  as shown in Fig. 7. Figure 8 is plotted to examine the behavior of Eckert number  $Ec_x$  against temperature  $\theta(\eta)$ , since  $Ec_x$  is a relation between kinetic energy and enthalpy, increase in  $Ec_x$  causes increase of kinetic energy which further rises up the molecular motion and hence temperature rises. Figure 9 is sketched to see the variation of radiation parameter

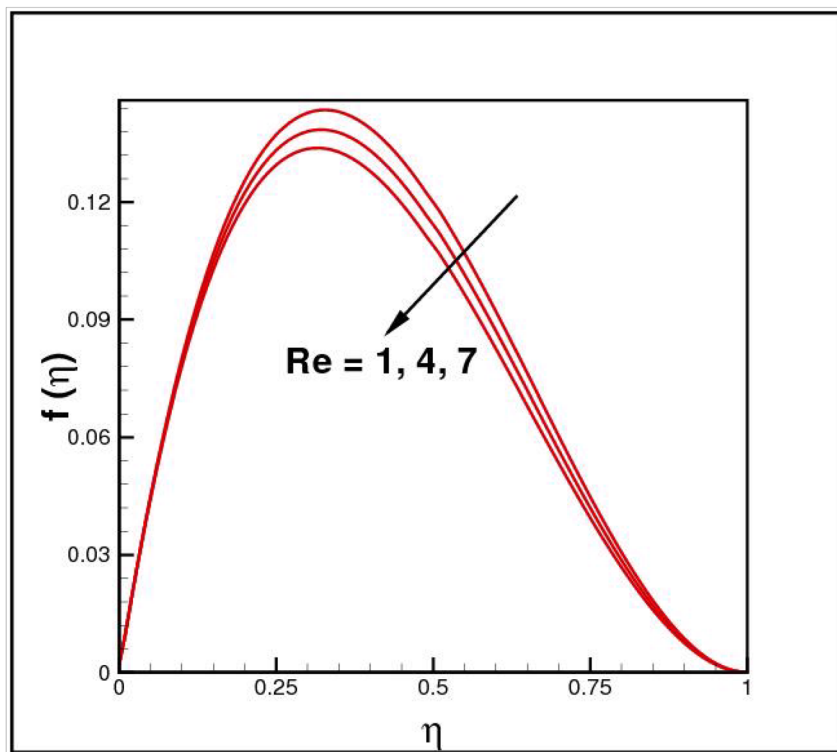


Figure 3. Impact of  $Re$  on  $f(\eta)$ .

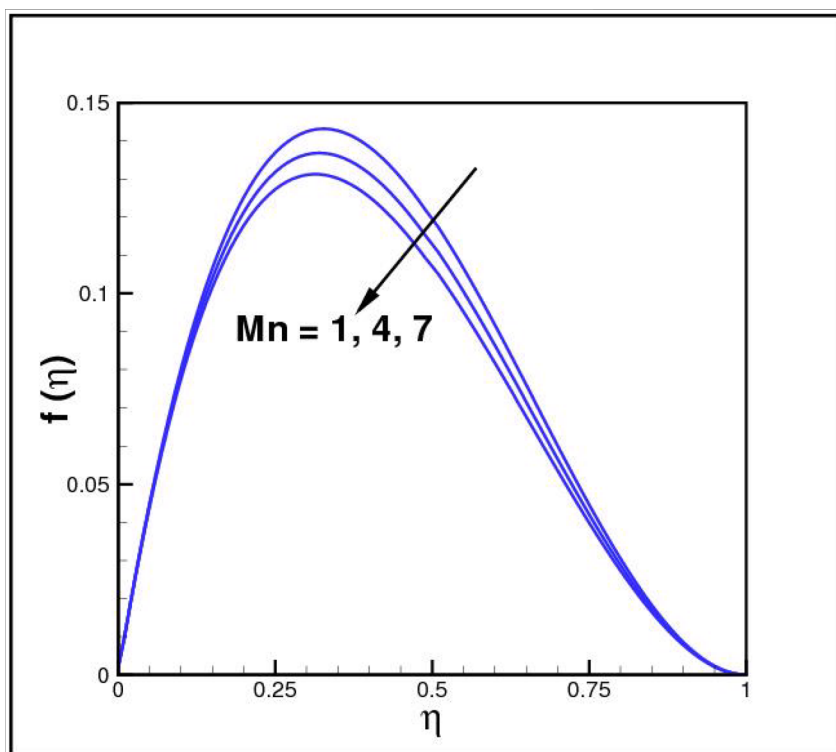


Figure 4. Impact of  $Mn$  on  $f(\eta)$ .

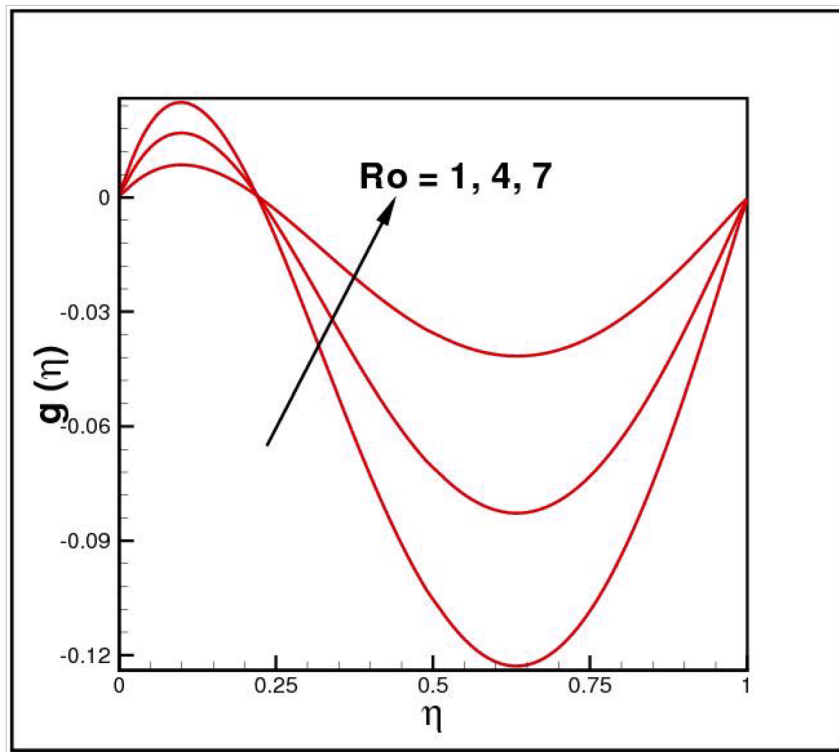


Figure 5. Impact of  $Ro$  on  $g(\eta)$ .

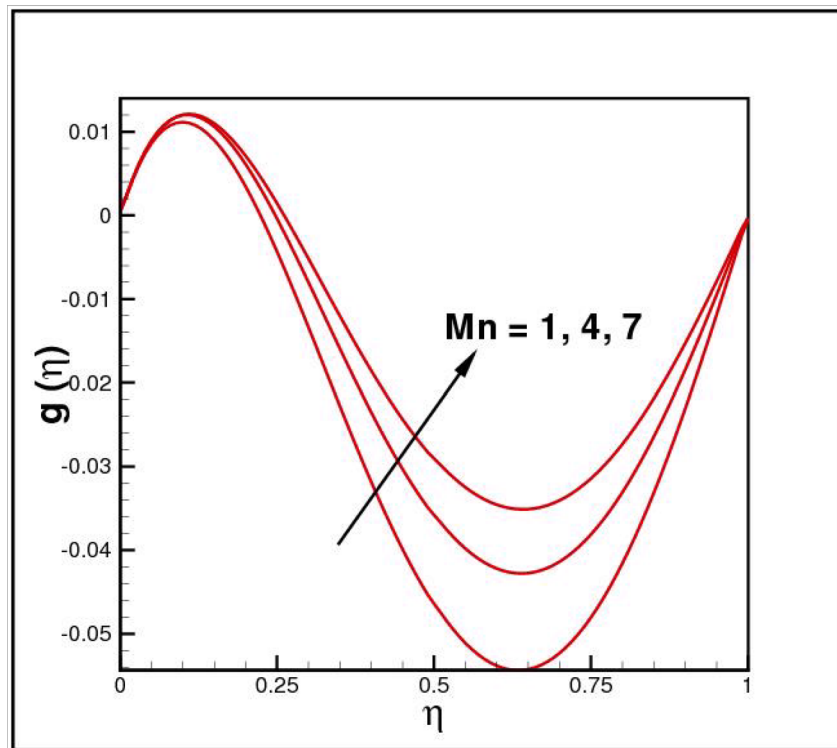


Figure 6. Impact of  $Mn$  on  $g(\eta)$ .

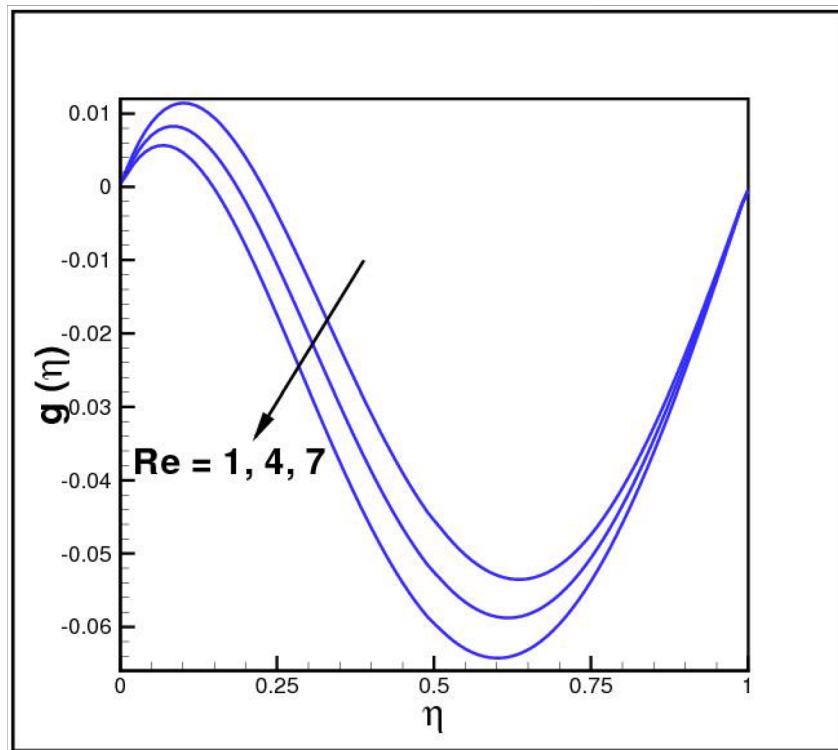


Figure 7. Impact of  $Re$  on  $g(\eta)$ .

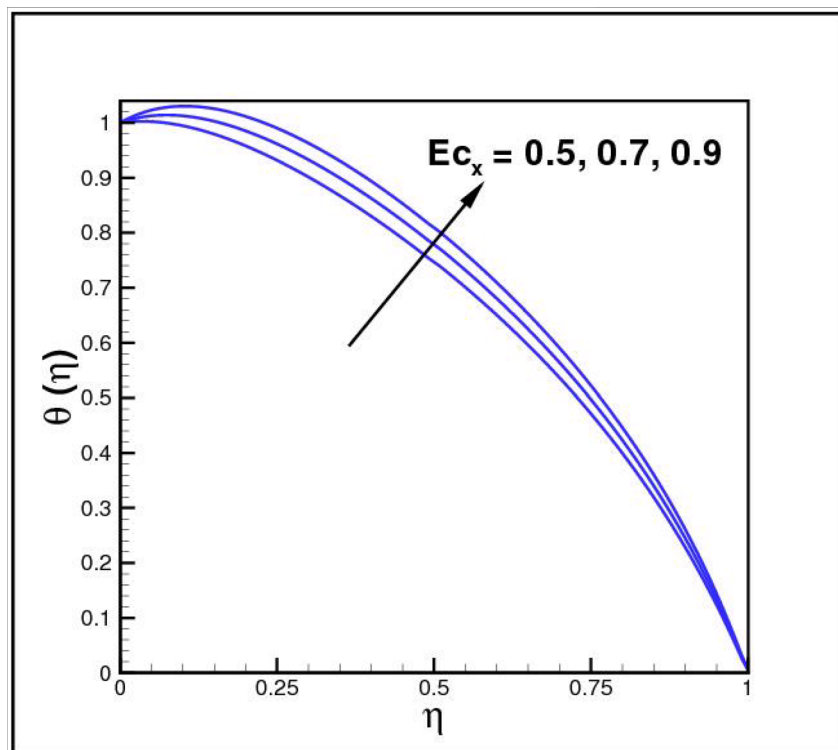


Figure 8. Impact of  $Ec_x$  on  $\theta(\eta)$ .



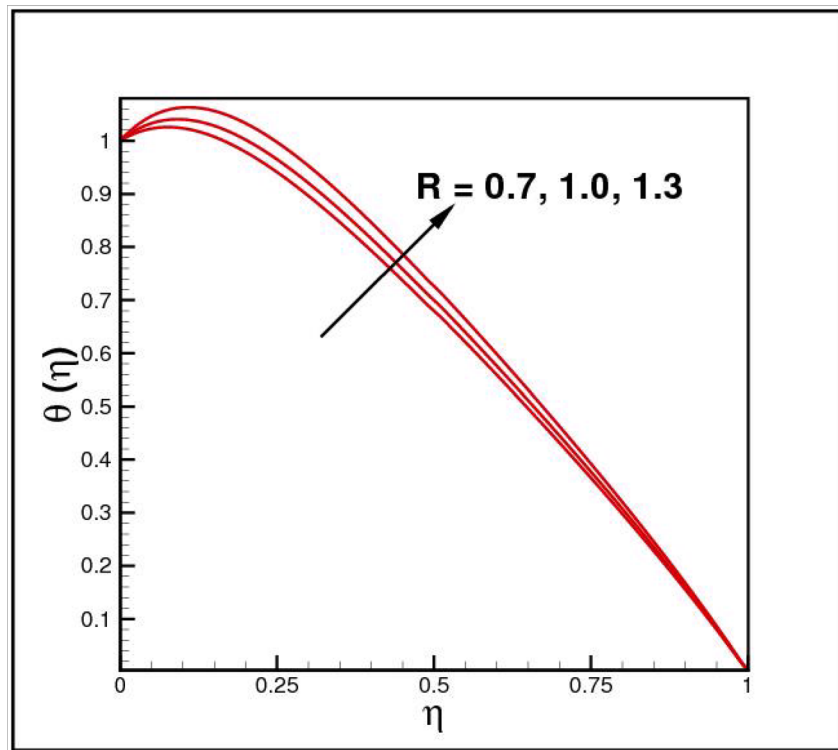


Figure 9. Impact of  $R$  on  $\theta(\eta)$ .

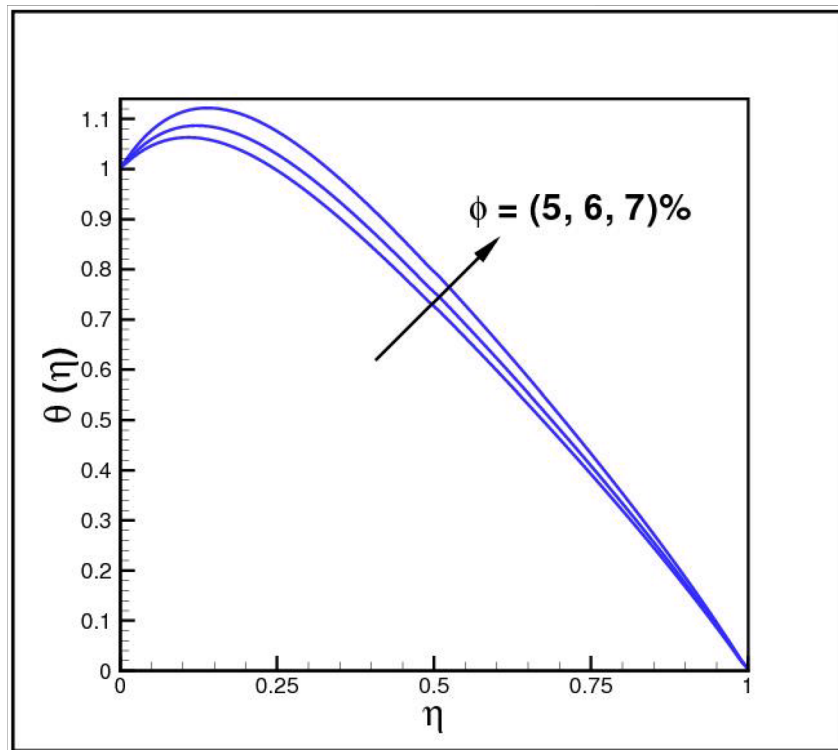


Figure 10. Impact of  $\phi$  on  $\theta(\eta)$ .

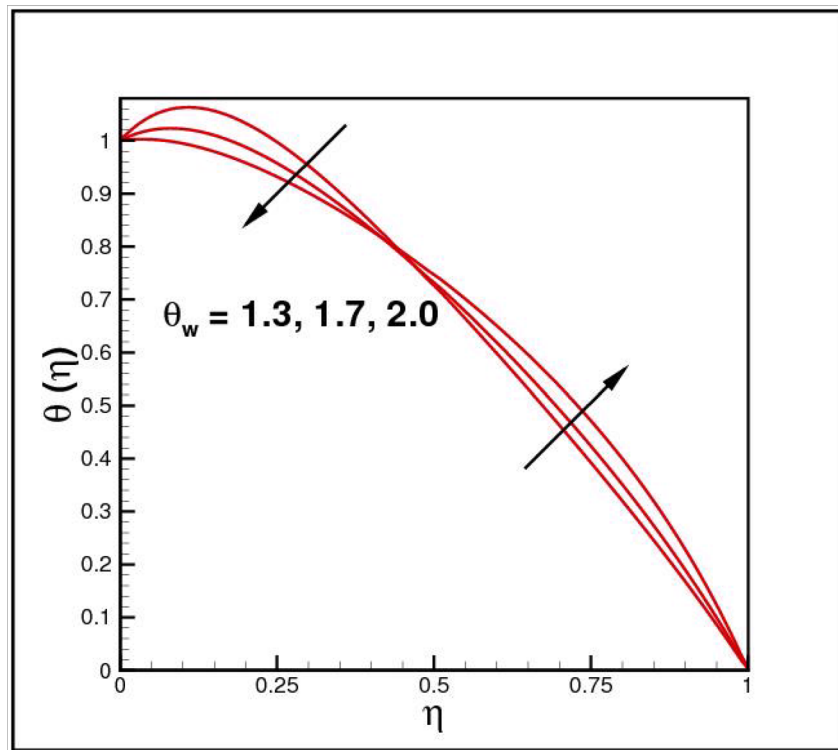


Figure 11. Impact of  $\theta_w$  on  $\theta(\eta)$ .

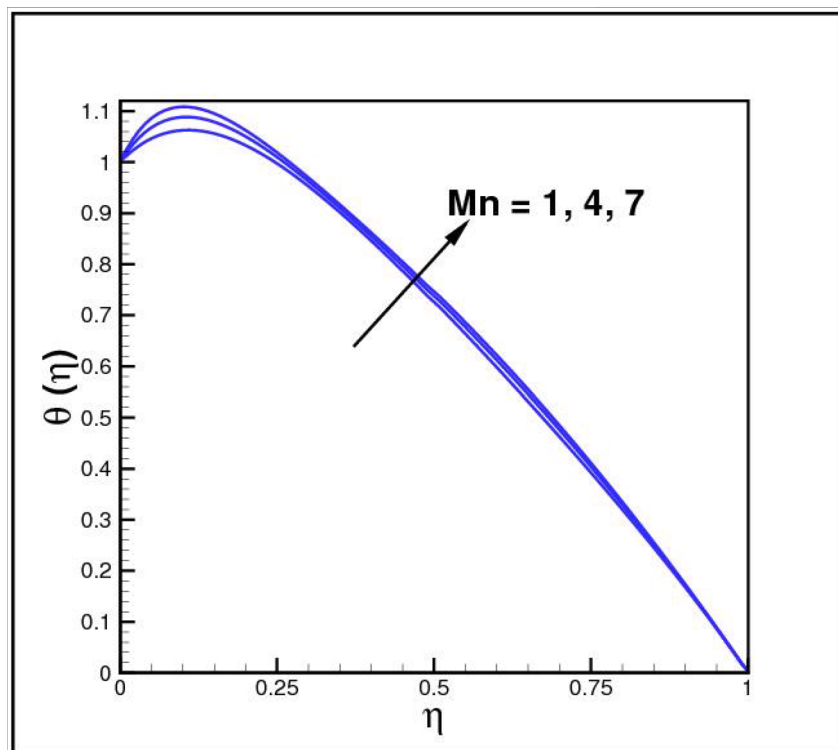


Figure 12. Impact of  $Mn$  on  $\theta(\eta)$ .

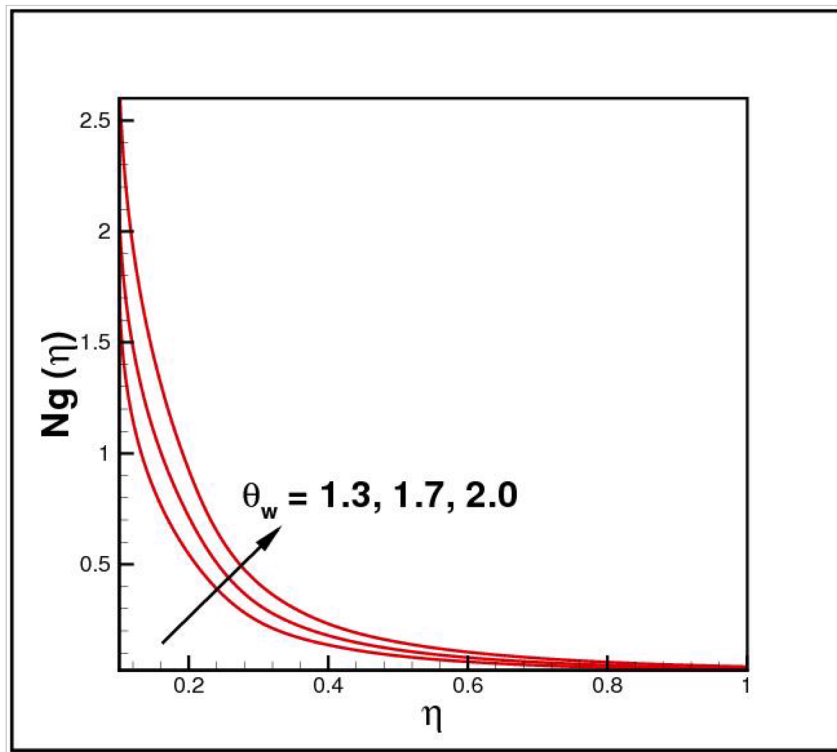


Figure 13. Impact of  $\theta_w$  on  $Ng(\eta)$ .

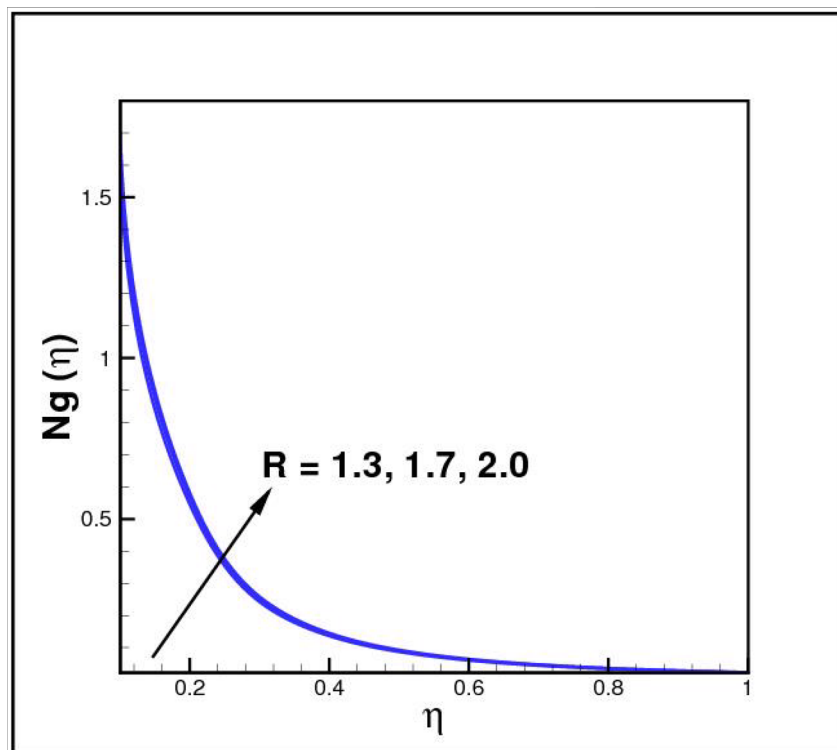
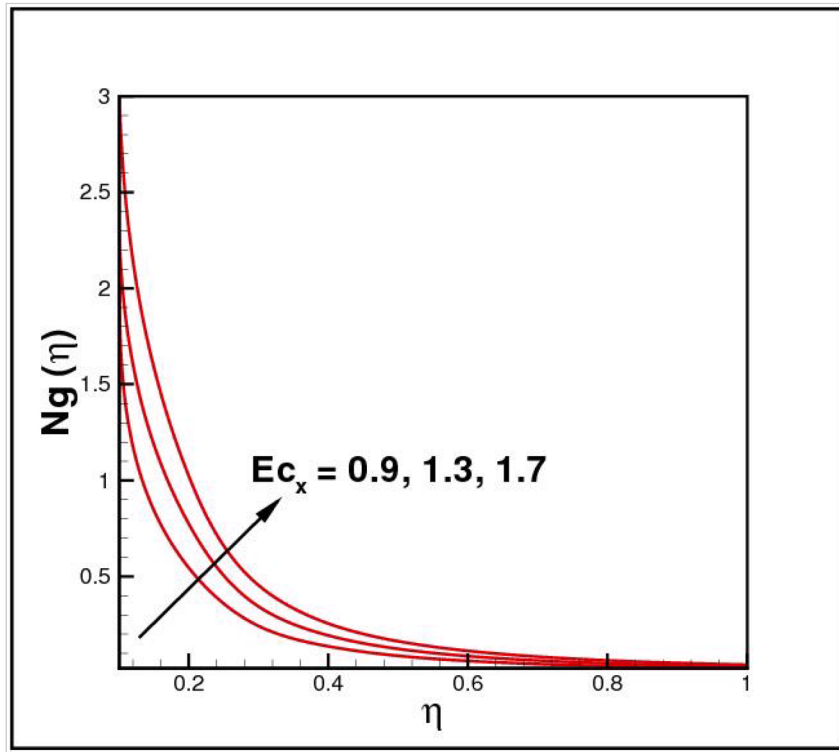


Figure 14. Impact of  $R$  on  $Ng(\eta)$ .



**Figure 15.** Impact of  $Ec_x$  on  $Ng(\eta)$ .

$R$  on temperature  $\theta(\eta)$ . It is observed that  $\theta(\eta)$  enhanced versus higher  $R$ . Figure 10 plots the temperature  $\theta(\eta)$  for various percentages of volume fraction of nanoparticles  $\phi$ . Clearly  $\theta(\eta)$  enhances with an increase in  $\phi$ . From Fig. 11 it is observed that for higher estimates of temperature ratio parameter  $\theta_w$ , temperature  $\theta(\eta)$  inclines near the lower surface while declines near upper boundary. Figure 12 shows the effect of magnetic parameter  $Mn$  on temperature  $\theta(\eta)$ , since  $Mn$  is a resistive body force hence larger  $Mn$  causes increment in  $\theta(\eta)$ . Figures 13, 14 and 15 exhibit the dimensionless entropy generation  $Ng(\eta)$  for different values of temperature ratio parameter  $\theta_w$ , radiation parameter  $R$  and Eckert number  $Ec_x$  respectively. An enhancement is observed in  $Ng(\eta)$  versus higher values of all parameters. Figure 16 describes the variation in surface drag force  $C_f(\eta)$  due to volume fraction of nanoparticles  $\phi$ . Here higher  $\phi$  reasons lower  $C_f(\eta)$ . Figure 17 demonstrates the impact of Reynolds number  $Re$  against  $C_f(\eta)$ . Clearly  $C_f(\eta)$  shows increasing behavior for larger  $Re$ . Figures 18 and 19 explored effects of temperature ratio parameter  $\theta_w$  and radiation parameter  $R$  on Nusselt number  $Nu(\eta)$ . Increment in  $Nu(\eta)$  is noticed for the higher values of both parameters.

Table 2 is constructed for the comparative analysis of present work with Ishak et al.<sup>21</sup> and observed very good agreement with them.

### Concluding remarks

Here the flow analysis of  $Ag - Cu/EG$  hybrid nanofluid is discussed. Key findings are listed below.

- Velocity  $f(\eta)$  is the decreasing function of higher  $Re$  and  $Mn$ .
- Velocity  $g(\eta)$  enhances against higher  $Mn$  while it decays against the estimation of  $Re$ .
- Increment in temperature  $\theta(\eta)$  is seen for higher  $R$  and  $Mn$ .
- $C_f$  is enhanced for  $Re$  while it declined against  $\phi$ .
- $Ng(\eta)$  rises versus higher  $Ec_x$ .
- Magnitude of  $Nu$  is an increasing function of  $R$  and  $\theta_w$ .

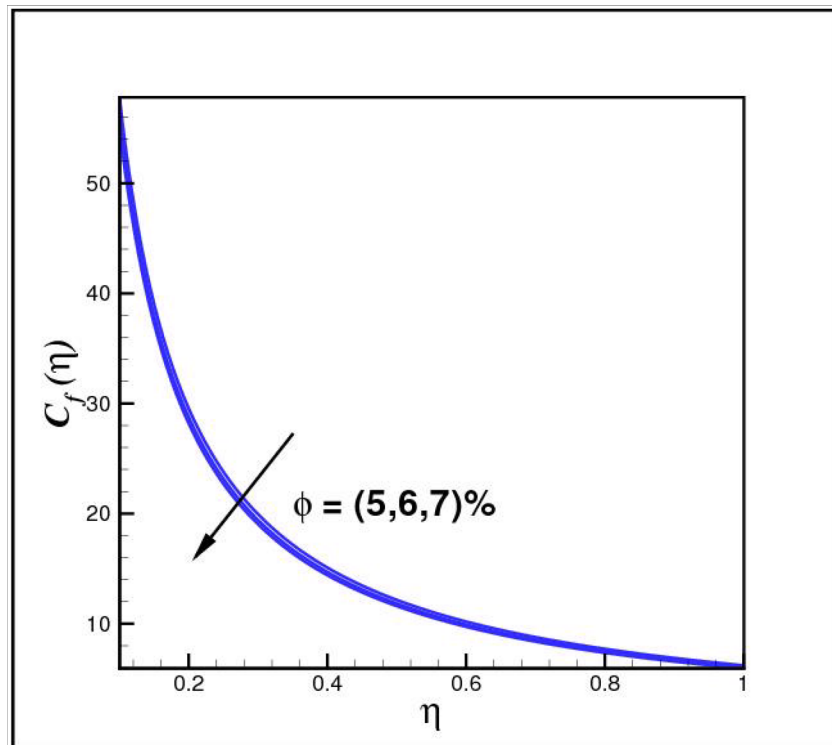


Figure 16. Impact of  $\phi$  on  $C_f(\eta)$ .

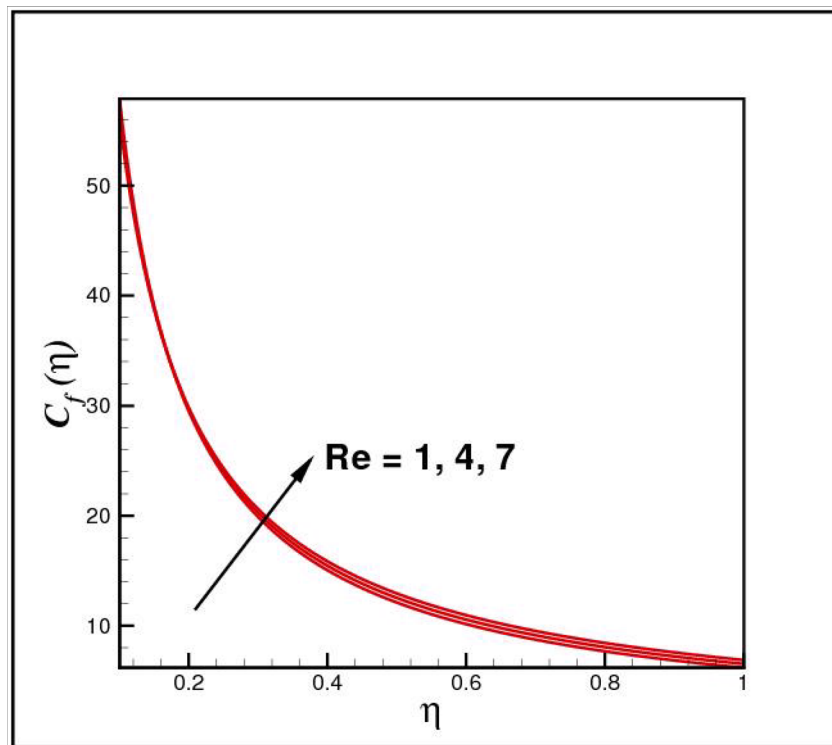
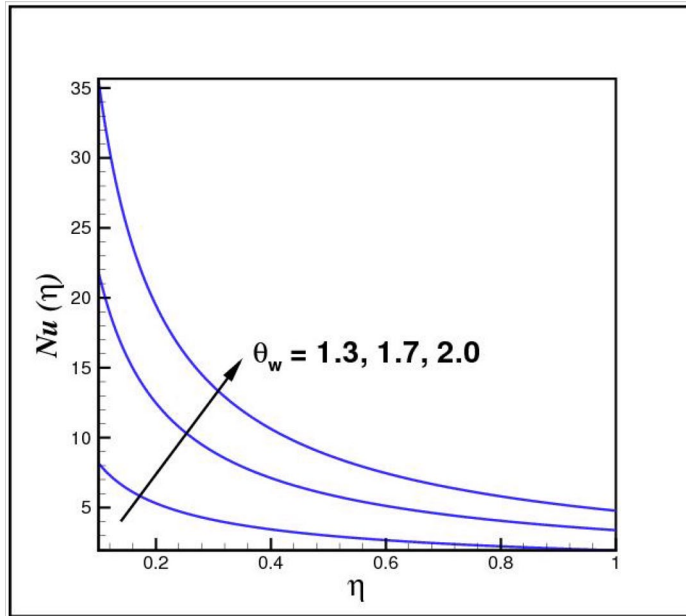
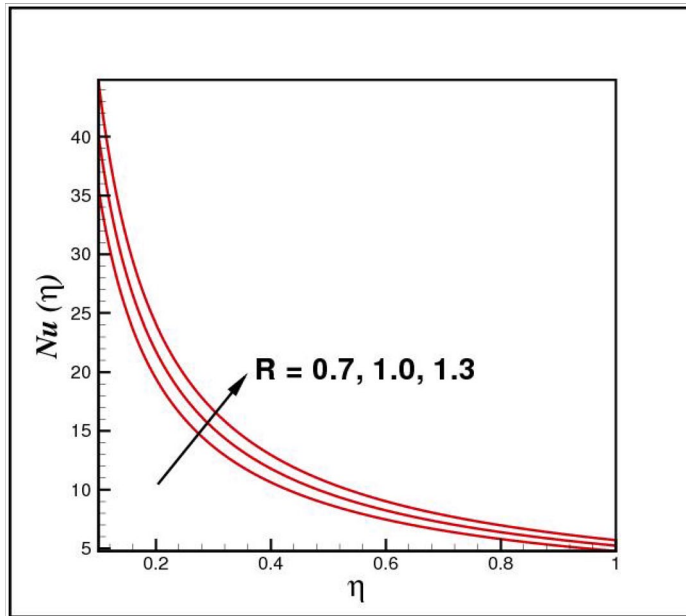


Figure 17. Impact of  $Re$  on  $C_f(\eta)$ .



**Figure 18.** Impact of  $\theta_w$  on  $Nu(\eta)$ .



**Figure 19.** Impact of  $R$  on  $Nu(\eta)$ .

**Data availability**

The data that support the findings of this study are available within the article, the data are made by the authors themselves and do not involve references of others.

Received: 1 May 2021; Accepted: 13 July 2021

Published online: 09 August 2021

**References**

1. Hayat, T., Abbas, Z. & Sajid, M. MHD stagnation-point flow of an upper-convected Maxwell fluid over a stretching surface. *Chaos Solitons Fract.* **39**(2), 840–848 (2009).
2. Andersson, H. I. MHD flow of a viscoelastic fluid past a stretching surface. *Acta Mech.* **95**(1–4), 227–230 (1992).

3. El-Kabeir, S. M. M., Chamkha, A. & Rashad, A. M. Heat and mass transfer by MHD stagnation-point flow of a power-law fluid towards a stretching surface with radiation, chemical reaction and Soret and Dufour effects. *Int. J. Chem. React. Eng.* **8**(1), A132 (2010).
4. Hayat, T., Khan, M. I., Qayyum, S., Alsaedi, A. & Khan, M. I. New thermodynamics of entropy generation minimization with nonlinear thermal radiation and nanomaterials. *Phys. Lett. A* **382**(11), 749–760 (2018).
5. Shehzad, S. A., Hayat, T., Alsaedi, A. & Obid, M. A. Nonlinear thermal radiation in three-dimensional flow of Jeffrey nanofluid: A model for solar energy. *Appl. Math. Comput.* **248**, 273–286 (2014).
6. Waqas, M., Khan, M. I., Hayat, T., Alsaedi, A. & Khan, M. I. Nonlinear thermal radiation in flow induced by a slendering surface accounting thermophoresis and Brownian diffusion. *Eur. Phys. J. Plus* **132**(6), 280 (2017).
7. Kumar, R., Sood, S., Sheikholeslami, M. & Shehzad, S. A. Nonlinear thermal radiation and cubic autocatalysis chemical reaction effects on the flow of stretched nanofluid under rotational oscillations. *J. Colloid Interface Sci.* **505**, 253–265 (2017).
8. Gebhart, B. Effects of viscous dissipation in natural convection. *J. Fluid Mech.* **14**(2), 225–232 (1962).
9. Koo, J. & Kleinstreuer, C. Viscous dissipation effects in microtubes and microchannels. *Int. J. Heat Mass Transf.* **47**(14–16), 3159–3169 (2004).
10. Hayat, T., Khan, M. I., Waqas, M., Yasmeen, T. & Alsaedi, A. Viscous dissipation effect in flow of magnetonanofluid with variable properties. *J. Mol. Liq.* **222**, 47–54 (2016).
11. Mustafa, M., Hayat, T. & Hendi, A. A. Influence of melting heat transfer in the stagnation-point flow of a Jeffrey fluid in the presence of viscous dissipation. *J. Appl. Mech.* **79**(2), 024501 (2012).
12. Bejan, A. A study of entropy generation in fundamental convective heat transfer. *J. Heat Transf.* **101**(4), 718–725 (1979).
13. Rashidi, M. M., Abelman, S. & Mehr, N. F. Entropy generation in steady MHD flow due to a rotating porous disk in a nanofluid. *Int. J. Heat Mass Transf.* **62**, 515–525 (2013).
14. Hayat, T., Khan, M. I., Qayyum, S. & Alsaedi, A. Entropy generation in flow with silver and copper nanoparticle. *Colloids Surf. A* **539**, 335–346 (2018).
15. Choi, S. U. S. & Eastman, J. A. Enhancing thermal conductivity of fluids with nanoparticles (No. ANL/MSD/CP-84938; CONF-951135-29), Argonne National Lab, IL (United States) (1995).
16. Prasher, R., Song, D., Wang, J. & Phelan, P. Measurements of nanofluid viscosity and its implications for thermal applications. *Appl. Phys. Lett.* **89**(13), 133108 (2006).
17. Sheikholeslami, M., Rashidi, M. M., Hayat, T. & Ganji, D. D. Free convection of magnetic nanofluid considering MFD viscosity effect. *J. Mol. Liq.* **218**, 393–399 (2016).
18. Khan, M. I., Hafeez, M. U., Hayat, T., Khan, M. I. & Alsaedi, A. Magneto rotating flow of hybrid nanofluid with entropy generation. *Comput. Methods Progr. Biomed.* **183**, 105093 (2020).
19. Chamkha, A. J., Dogonchi, A. S. & Ganji, D. D. Magneto-hydrodynamic flow and heat transfer of a hybrid nanofluid in a rotating system among two surfaces in the presence of thermal radiation and Joule heating. *AIP Adv.* **9**(2), 025103 (2019).
20. Hayat, T. & Nadeem, S. Heat transfer enhancement with hybrid nanofluid. *Results Phys.* **7**, 2317–2324 (2017).
21. Ishak, A., Nazar, R. & Pop, I. Heat transfer over an unsteady stretching permeable surface with prescribed wall temperature. *Nonlinear Anal. R. World Appl.* **10**, 2909–2913 (2009).
22. Hayat, T., Kiran, A., Imtiaz, M. & Alsaedi, A. Hydromagnetic mixed convection flow of copper and silver water nanofluids due to a curved stretching sheet. *Results Phys.* **6**, 904–910 (2016).
23. Hafeez, M. U., Hayat, T., Alsaedi, A. & Khan, M. I. Numerical simulation for electrical conducting rotating flow of Au (Gold)–Zn (Zinc)/EG (Ethylene glycol) hybrid nanofluid. *Int. Commun. Heat Mass Transf.* **124**, 105234 (2021).
24. Acharya, N., Bag, R. & Kundu, P. K. Influence of Hall current on radiative nanofluid flow over a spinning disk: A hybrid approach. *Phys. E* **111**, 103–112 (2019).
25. Hayat, T., Qayyum, S., Khan, M. I. & Alsaedi, A. Current progresses about probable error and statistical declaration for radiative two phase flow using AgH<sub>2</sub>O and CuH<sub>2</sub>O nanomaterials. *Int. J. Hydrogen Energy* **42**, 29107–29120 (2017).
26. Acharya, N. Spectral quasi linearization simulation of radiative nanofluidic transport over a bended surface considering the effects of multiple convective conditions. *Eur. J. Mech. B Fluid* **84**, 139–154 (2020).
27. Acharya, N., Maity, S. & Kundu, P. K. Influence of inclined magnetic field on the flow of condensed nanomaterial over a slippery surface: The hybrid visualization. *Appl. Nanosci.* **10**, 633–647 (2020).
28. Yasmeen, T., Hayat, T., Khan, M. I., Imtiaz, M. & Alsaedi, A. Ferrofluid flow by a stretched surface in the presence of magnetic dipole and homogeneous–heterogeneous reactions. *J. Mol. Liq.* **223**, 1000–1005 (2016).
29. Acharya, N., Bag, R. & Kundu, P. K. On the impact of nonlinear thermal radiation on magnetized hybrid condensed nanofluid flow over a permeable texture. *Appl. Nanosci.* **10**, 1679–1691 (2020).
30. Acharya, N. On the flow patterns and thermal behaviour of hybrid nanofluid flow inside a microchannel in presence of radiative solar energy. *J. Therm. Anal. Calorim.* **141**, 1425–1442 (2020).

## Acknowledgements

This research was supported by Basic Science Research Program through the National Research Foundation of Korea (NRF) funded by the Ministry of Education (No. 2017R1D1A1B05030422).

## Author contributions

The research work of the subject paper was performed under the supervision of Principle investigator Dr. M. I.K. The author M.U.H. has done formal analysis and software packages respectively. The author W.-F.X. has addressed the reviewer comments and re-written the final draft. The authors N.A.S. and J.D.C. have reviewed and edited the final version. Further, the results are improved and compared with previous literature as suggested by reviewers are done through these authors.

## Competing interests

The authors declare no competing interests.

## Additional information

**Correspondence** and requests for materials should be addressed to N.A.S.

**Reprints and permissions information** is available at [www.nature.com/reprints](http://www.nature.com/reprints).

**Publisher's note** Springer Nature remains neutral with regard to jurisdictional claims in published maps and institutional affiliations.



**Open Access** This article is licensed under a Creative Commons Attribution 4.0 International License, which permits use, sharing, adaptation, distribution and reproduction in any medium or format, as long as you give appropriate credit to the original author(s) and the source, provide a link to the Creative Commons licence, and indicate if changes were made. The images or other third party material in this article are included in the article's Creative Commons licence, unless indicated otherwise in a credit line to the material. If material is not included in the article's Creative Commons licence and your intended use is not permitted by statutory regulation or exceeds the permitted use, you will need to obtain permission directly from the copyright holder. To view a copy of this licence, visit <http://creativecommons.org/licenses/by/4.0/>.

© The Author(s) 2021